Article

pubs.acs.org/Biomac

Suppressing Unspecific Cell Uptake for Targeted Delivery Using Hydroxyethyl Starch Nanocapsules

Grit Baier, Daniela Baumann, Jörg Max Siebert, Anna Musyanovych, Volker Mailänder, and Katharina Landfester*

Max Planck Institute for Polymer Research, Ackermannweg 10, 55128 Mainz, Germany

Supporting Information

ABSTRACT: Synthesizing nanocarriers with stealth properties and delivering a "payload" to the particular organ remains a big challenge but is the prime prerequisite for any in vivo application. As a nontoxic alternative to the modification by poly(ethylene glycol) PEG, we describe the synthesis of cross-linked hydroxyethyl starch (HES, M_w 200,000 g/mol) nanocapsules with a size range of 170−300 nm, which do not show nonspecific uptake into cells. The specific uptake was shown by coupling a folic acid conjugate as a model targeting agent onto the surface of the nanocapsules, because folic acid has a high affinity to a variety of human carcinoma cell lines which overexpress the folate receptor on the cell surface. The covalent binding of the folic acid conjugate onto HES capsules was confirmed by FTIR and NMR spectroscopy. The coupling efficiency was determined using fluorescence spectroscopy. The specific cellular uptake of the HES nanocapsules after folic acid coupling into the folate-receptor presenting cells was studied by confocal laser scanning microscopy (CLSM) and flow cytometry.

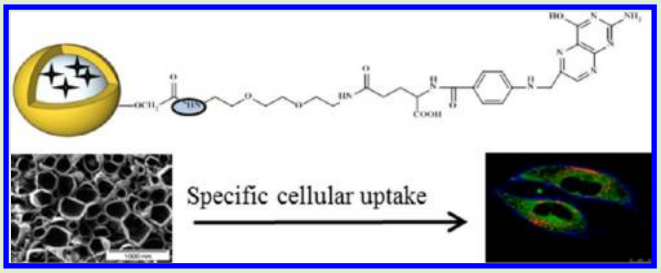

INTRODUCTION

In recent years, the use of nanoparticles in cell imaging,[1−3] drug delivery,[4,5] diagnostics, and therapy[6,7] have received significant attention in the biomedical community. Extensive efforts have been devoted to produce nanocarriers that possess low toxicity, a high affinity to target cells, and an avoidance of unspecific uptake and also provide an effective protection of therapeutic agents against chemical and enzymatic degradation.[8−13] The use of biodegradable polymers derived from natural sources in the formation of nanocarriers has a big advantage over synthetic polymers.

To be able to obtain targeting nanocarriers, the nonspecific interaction and uptake of the nanoparticles into nontarget cells should be minimized; the specificity to the target tissue or cell type can be obtained by molecules (or ligands) that are coupled to the nanocarrier and interact specifically with the target structures in the tissue by, for example, ligand−receptor or antibody−antigen interactions.

Folic acid has a high affinity to folate receptors which are overexpressed (mainly FRα) on the surface of various tumor carcinoma cells, such as osteosarcoma, non-Hodgkin lymphoma, and leukemia. A limited tissue distribution of these receptors is found in normal cells.[6] This overexpression turns folic acid into an important marker for a targeted release of molecules into these cells.[4,14] Folic acid has been studied extensively as a targeting molecule for different therapeutic and imaging agents for cancer treatment.[5,8,9,12] The binding affinity of folic acid to FRα is around 10 times higher compared to that of folate derivatives.[15]

The nonspecific uptake can be considerably reduced by using poly(ethylene glycol) (PEG) chains at the surface of nanoparticles. However, PEG shows toxicity at high, parenteral doses and in long-term use. The usual target organ is the kidney as this is the route of excretion for PEG.[16] Biocompatible hydroxyethyl starch (HES) is a naturally derived substitute for the often used synthetic water-soluble PEG.[17] In general, polysaccharides have proven to be a good alternative for the reduction or prevention of protein adsorption.[18,19]

HES is a hydroxyethylated glucose polymer that is used in medicine for the treatment of hypovolemic shock, artery occlusive disease, cerebral ischemia, or apoplectic insult, respectively, because HES improves the microcirculation within the organism, due to the improvement of blood viscosity.[20−22] The retention time of HES within the blood plasma (vascular compartment), liver, lungs, spleen, and reticuloendothelial system (RES) is significantly higher compared to native starch and, with increasing molar substitution, the enzymatic degradation and the renal elimination time is prolonged.[23−25] Animal testing showed that the activity of serum amylase for intravascular enzymatic cleavage is of less importance than the intracellular cleavage after phagocytosis.[26]

The interaction between poly(lactic-*co*-glycolic acid) (PLGA) particles stabilized with HES and phagocytic cells was compared with the interaction of the same cells with

Received: April 26, 2012
Revised: July 25, 2012
Published: July 30, 2012

dx.doi.org/10.1021/bm300653v | *Biomacromolecules* 2012, 13, 2704−2715

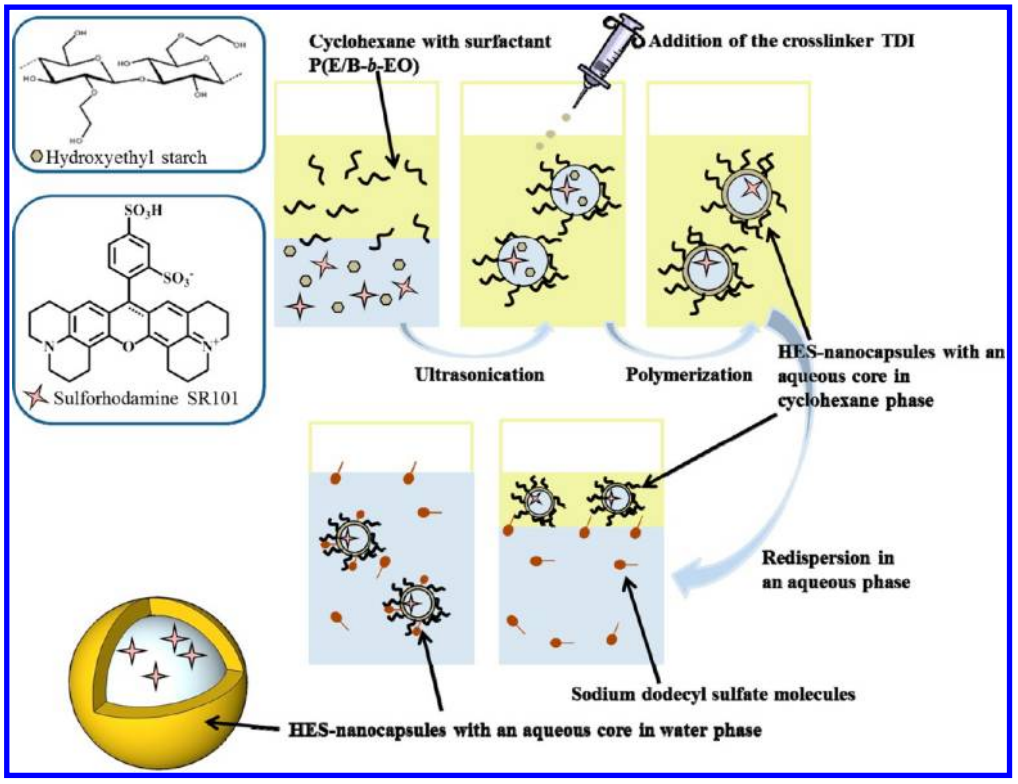

Figure 1. Scheme of the synthesis and redispersion of the HES nanocapsules using the inverse (water-in-oil) miniemulsion process.

pluronic-stabilized PLGA particles and revealed a reduction in the cell uptake of HES-stabilized particles.[17]

In principle, polymeric HES particles or capsules are very suitable for the encapsulation of various biomolecules, due to the biological tolerance and degradability, shelf life, high loading capacity, and the possibility of a targeted release.[27] Bajpai and Bhanu reported on the controlled release of heparin out of glutaraldehyde cross-linked starch microspheres with a diameter range of 5−11 μm synthesized by the solvent evaporation technique.[28] In other publications, the synthesis of HES microcapsules cross-linked with terephthaloyl chloride (diameter range of 4−15 μm) containing bovine serum albumin (BSA) was described.[27,29] The obtained microcapsules were subjected to the enzymatic release studies performed in vitro using melanoma cells and in vivo after intraperitoneal application. For intravenous drug delivery, HES is more beneficial compared to natural starch, which is enzymatically unstable and degrades by amylase within 2 h.[30]

For intravenous drug delivery applications and possible cell uptake, the nanocarriers have to be much smaller, preferably below 300 nm. One of the advantages of using nanocapsules as site-specific carriers is that they can deliver a high amount of therapeutic molecules. For the formation of stable polymeric nanocapsules with an aqueous core, the inverse miniemulsion has been shown to be a very versatile technique that also allows the use of polymers and biomolecules for the shell formation.[31]

In this present contribution, HES nanocapsules with low nonspecific uptake behavior into cells with a size below 300 nm were obtained through an interfacial polyaddition reaction with diisocyanate in an inverse miniemulsion. After redispersion in water, the residual hydroxyl end-groups of the polyurethane on the capsule's surface were converted to carboxylic groups by the carboxymethylation procedure.[32] As model targeting molecule folic acid (vitamin B_9) which consists of a pteridine derivative, *para*-aminobenzoic acid, and L-glutamine acid was covalently attached to the HES nanocapsules. The highest receptor affinity and receptor-mediated endocytosis is achieved when binding the γ-carboxyl group of the folic acid to the other molecule using a covalent link.[4,33−35] Folic acid was covalently linked (via γ-carboxyl group) to the NH_2 terminated conjugate, which is used for coupling with the carboxylic groups on the HES nanocapsules surface. In consequence, the folic acid should completely retain its physiological properties and binding affinity to FRα. HeLa cells, a human cervix carcinoma cell line, were used as FRα positive cells, and A549 cells served as FRα nonexpressing cell line. A potential folic acid receptor-mediated cellular uptake pathway was analyzed. We believe that the results presented in this work will be of great interest for the development of nanocarriers for active receptor-mediated targeting by providing a platform that avoids nonspecific uptake into nontarget cells and therefore provides an alternative to PEGylation.

EXPERIMENTAL SECTION

Materials. All chemicals or materials were used without further purification. The hydroxyethyl starch (HES, M_w =200000 g·mol^{-1}) was purchased from Fresenius Kabi. 2,4-Toluene diisocyanate (TDI) and cyclohexane (>99.9%) were purchased from Sigma Aldrich. The oil-soluble surfactant poly((ethylene-*co*-butylene)-*b*-(ethylene oxide)), P(E/B-*b*-EO), consisting of a poly(ethylene-*co*-butylene) block (M_w = 3700 g·mol^{-1}) and a poly(ethylene oxide) block (M_w = 3600 g·mol^{-1}) was synthesized starting from ω-hydroxypoly(ethylene-*co*-butylene), which was dissolved in toluene after addition of ethylene oxide under anionic polymerization conditions.[36] The anionic surfactant sodium dodecylsulfate (SDS) was purchased from Fluka. The fluorescent dye sulforhodamine 101 (SR101) (M = 606.71 g·mol^{-1}) was purchased from BioChemica, Aldrich. *N*-Ethyl-*N*′-(3-dimethylaminopropyl)-carbodiimide (EDC), *N*-hydroxysulfosuccinimide (sulfo-NHS), and monochloroacetic acid (MCA) were purchased from Aldrich and folic acid was purchased from SERVA. Dimethylsulfoxide (<50 ppm water

dx.doi.org/10.1021/bm300653v | *Biomacromolecules* 2012, 13, 2704−2715

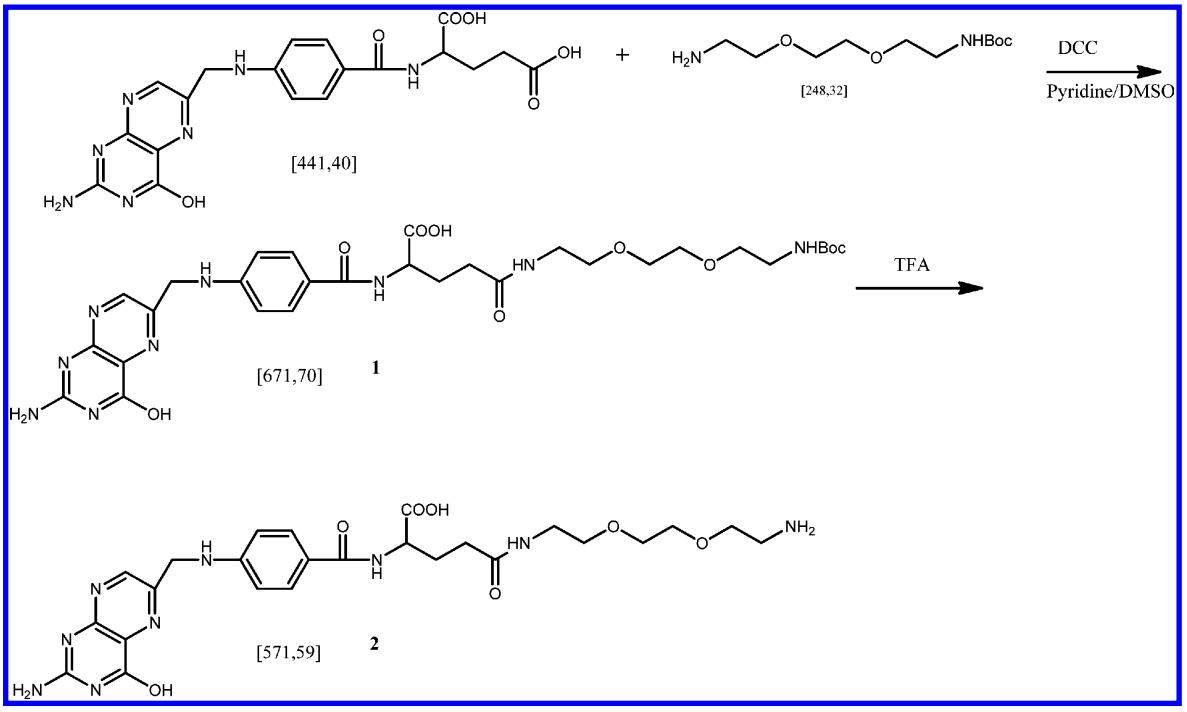

Figure 2. Synthesis of the NH_2-terminated folic acid conjugate.

content) and pyridine (99.5%, < 50 ppm water content) were purchased from Acros Organics. Dicyclocarbodiimide (99%), trifluoracetic acid (99%), and *tert*-butyl 2-[2-(2-aminoethoxy)ethoxy]-ethylcarbamate (>95%) were purchased from Sigma-Aldrich.

Preparation of HES Nanocapsules. The HES nanocapsules were prepared by a polyaddition reaction performed at the miniemulsion droplet's interface similar to the previously published procedure,[31,37,38] see Figure 1. Briefly, 1400 mg of an aqueous HES (100 mg·mL^{-1}) solution were mixed with the fluorescent dye sulforhodamine 101 (2 mM; mixture I). Then 100 mg of the surfactant P(E/B-*b*-EO) were dissolved in 7.5 g cyclohexane, added to mixture I and stirred over 1 h at 25 °C. After the homogenization step (ultrasonication: 180 s at 70% amplitude in a pulse regime (20 s sonication, 10 s pause) using a Branson Sonifier W-450-Digital and a 1/2″ tip under ice cooling) a clear solution consisting of 5 g cyclohexane, 30 mg P(E/B-*b*-EO), and 100 mg of TDI was added dropwise over 5 min to the earlier prepared mixture I at 25 °C. The reaction was performed for 20 h at 25 °C under stirring. After synthesis, nanocapsules were purified by repetitive centrifugation (Sigma 3k-30, RCF 3300, 20 min, two times) to remove the residues of surfactant and redispersed in cyclohexane. Afterward, the nanocapsules were transferred into the aqueous phase using the following procedure: 1 g of the nanocapsules dispersion in cyclohexane (polymer solid content around 3 wt %) was mixed with 5 g SDS aqueous solution (0.1 wt %) under mechanical stirring for 24 h at 25 °C. Then, the samples were redispersed for 5 min at 50 °C in a sonication bath (power 50%, 25 kHz). After redispersion the nanocapsules were centrifuged at 4000 rpm for 20 min (Sigma 3k-30, RCF 1467) and dialyzed (MWCO: 12000 g·mol^{-1}) to remove residues of SDS. The supernatant was removed and the pellet was resuspended in demineralized water.

Determination of the Polymeric HES Nanocapsules Permeability. The permeability of the capsules' shells was studied on SR101-containing capsules redispersed in water using a fluorescence spectrometer (NanoDrop ND-3300, PEQLab). The fluorescent dye SR101 absorbs light at 550 nm and emits light at 605 nm. After the encapsulation and the redispersion process the polymeric nanocapsules were sedimented by centrifugation (at 4000 rpm for 20 min using Sigma 3k-30, RCF 1467). The nanocapsules prepared without fluorescent dye, but redispersed in an aqueous SDS solution containing SR101 (the amount is equal to SR101 amount taken in the encapsulation experiments), were used as a control sample. The total release of SR101 from the capsules was calculated as a difference between the fluorescent intensities of the supernatant obtained from the sample and the control sample. The fluorescence signal of the control sample was set as 100%. The polymeric nanocapsules were shaken gently for 40 d at 37 °C. After a given period of time, the amount of released SR101 was determined in the supernatant of the sedimented capsules and compared with the initial value. For each sample the encapsulation efficiency was calculated from six single measurements, and the whole experiment was repeated three times.

Carboxymethylation of HES Nanocapsules. The carboxymethylation of HES nanocapsules was performed using a modified procedure published previously.[32] Briefly, 4.0 g of HES nanocapsules aqueous dispersion (solid content 1.0 wt %) was mixed with 0.4 mL of NaOH solution (0.1 M) and stirred at 25 °C for 24 h to neutralize the nonreacted hydroxyl groups from the starch molecules on the nanocapsules surface. For the carboxymethylation, 40 μL of MCA (20.0 wt %) were mixed with the HES nanocapsules dispersion (after NaOH addition) and stirred for 24 h at 40 °C. After that 0.2 mL of a NaOH solution (1.0 M) was added and stirred again for 24 h at 25 °C. Finally, the nanocapsules dispersion was centrifuged (at 4000 rpm for 20 min, Sigma 3k-30, RCF 1467). The supernatant was removed. Nanocapsules were redispersed in demineralized water and the amount of carboxylic groups was determined by polyelectrolyte titration as described below.

Synthesis of NH_2 Terminated Folic Acid Conjugate. Synthesis of (*tert*-butyl *N*-(2-[2-(2-aminoethoxy)ethoxy]ethyl)carbamate) folic acid (**1**). The synthesis was performed according to Sahu et al.[5] with some modifications. A total of 1.47 g (3.33 mmol, 1.0 equiv) of folic acid was suspended in a predried nitrogen flask under argon atmosphere in 50 mL of DMSO and 20 mL of pyridine. A total of 1.36 g (6.66 mmol, 2.0 equiv) DCC (dicyclo-carbodiimide) was added and the resulting suspension was stirred for 30 min before 1.0 g (4 mmol, 1.2 equiv) *tert*-butyl 2-[2-(2-aminoethoxy)ethoxy]-ethylcarbamate was added. The resulting mixture was stirred for 18 h and subsequently filtrated through a D4 glass drip. The filtrate was poured into 200 mL of diethylether, filtrated, and the resulting yellow precipitate was thoroughly washed with cold diethylether. The yellow solid was dissolved in acetonitrile and precipitated again, pouring in diethylether. After drying in vacuum, 1.7 g (75%) of a yellow solid was obtained.

^{1}H NMR (DMSO-d_6, 300 MHz, δ in ppm): 1.36 (s, 9H), 1.8−2.3 (m, 4H), 2.96−3.41 (m, 8H), 3.46 (s, 2H), 3.52−3.56 (m, 2H), 4.19−4.38 (m, 1H), 4.47 (d, 2H, ^3J = 4.5 Hz), 6.64 (d, 2H, ^3J = 8.5 Hz), 6.76 (m, 1H), 6.92 (m, 1H), 7.08 (s, 1H), 7.64 (m, 2 H), 7.89 (m, 1H), 7.95 (s, 1H), 8.03 (m, 1H), 8.63 (s, 1H), 10.95 (s, 1H).

Synthesis of (*N*-(2-[2-(2-aminoethoxy)ethoxy]ethyl) folic acid (**2**). In a round-bottom flask, 1.5 g (2.2 mmol, 1.0 equiv) of **1** were mixed with 10 mL of TFA (trifluoracetic acid) and stirred for 2 h at 40 °C in a water bath. TFA was removed under reduced pressure and the remaining brownish gel was dissolved in 150 mL of water. The solution was poured into 800 mL of acetonitrile and a brownish precipitate was collected via filtration. The solid was dried under reduced pressure for 18 h at room temperature. Yield: 610 mg (50%). The reaction scheme is shown in Figure 2. The ^{1}H NMR spectrum of (*N*-(2-[2-(2-aminoethoxy)ethoxy]ethyl) folic acid is given in the Supporting Information, see Figure S2.

^{1}H NMR (DMSO-d_6, 300 MHz, δ in ppm): 1.88−2.07 (m, 2H), 2.19−2.31 (m, 2H), 2.95 (t, 1H, ^3J = 4.7 Hz), 3.17−3.42 (m, 6H), 3.48−3.61 (m, 5H), 4.29−4.36 (m, 1H), 4.48 (d, 2H, ^3J = 5.8 Hz), 6.64 (d, 8.7 Hz), 6.95 (m, 2H), 7.64 (m, 2H), 7.87−8.13 (m, 2H), 8.64 (s, 1H), 11.26 (s, 1H). FD-MS: 572 $(M + H)^+$ (100), 594 $(M + Na)^+$ (91), 610 $(M + K)^+$ (32).

Synthesis of Folic Acid-Conjugated HES Nanocapsules. Folic acid has two COOH groups positioned at the end of the molecule. The reactivity of γ-COOH is higher, and therefore, this group will react faster with NH_2 groups of the other molecules.[39] A 3.5 g aliquot of the carboxymethylated HES nanocapsules dispersion (solid content 1.0 wt %, 0.0045 mmol COOH groups) was mixed with 70 mg (0.45 mmol) EDC and 20 mg (0.09 mmol) sulfo-NHS to activate the carboxyl groups. After stirring for 30 min, the nanocapsules were centrifuged at 4000 rpm for 30 min (Sigma 3k-30, RCF 1467) to remove residuals of EDC and sulfo-NHS. The supernatant was removed and the pellet was resuspended in demineralized water. Then 30 mg (0.06 mmol) of NH_2-terminated folic acid conjugate were added and the mixture was stirred for another 12 h at ambient conditions. After the coupling procedure the nanocapsules were centrifuged at 4000 rpm for 20 min and dialyzed (MWCO: 12000 g·mol^{-1}) in order to remove residues of nonreacted NH_2-terminated folic acid conjugate.

Characterization of Folic Acid-Conjugated HES Nanocapsules. The amount of folic acid conjugate coupled to the HES nanocapsules was studied by measuring the fluorescence intensity using a plate reader (Infinite M1000, Tecan, Switzerland). A 3D-scan was performed to determine the absorption and emission signals of the folic acid conjugate. After the coupling procedure, the HES capsules were centrifuged (30 min at 4000 rpm) and the amount of folic acid conjugate present in the supernatant was calculated from the fluorescence intensity data. For the calculations, the calibration curve obtained with different amounts of dissolved folic acid conjugate was used.

Cell Culture. The cellular uptake of the HES nanocapsules before and after folic acid coupling was confirmed by confocal laser scanning microscopy (CLSM) and flow cytometry. Human cervix carcinoma cells (HeLa cells) and adenocarcinoma human alveolar basal epithelial cells (A549 cells) were kept in Dulbecco's Modified Eagle Medium (DMEM, Invitrogen, Germany). All were supplemented with 10% fetal calf serum (FCS), 100 units of penicillin, and 100 mg·mL^{-1} streptomycin, (all from Invitrogen, Germany). Cells were grown in a humidified incubator at 37 °C and 5% CO_2. On the day prior to the experiments, the adherent cells were detached by trypsin (Gibco, Germany) and seeded in a FCS-supplemented medium at a density of 50000 cells·cm^{-2} in six-well plates (Greiner, Germany) for flow cytometry and 10000 cells·cm^{-2} in ibiTreat μ-slides (IBIDI, Germany) for CLSM analysis. On the following day, HES nanocapsules (2.76×10^{13} nanocapsules per mL, labeled with SR101) were added to the medium in the presence of 10% FCS without using a transfection agent. Incubation periods had been carried out in a humidified incubator (37 °C, 5% CO_2). In the case of cellular uptake experiments carried out with and without additional folic acid in cell culture medium, cells were kept in folic acid free medium for a period of five days in total (for two consecutive passages) to stimulate the expression of membrane-anchored FRα. Three days before cell seeding, the standard DMEM medium was substituted by a folic acid free custom-made DMEM medium (Invitrogen, Germany), which included all other ingredients as in the standard DMEM medium. One day after cell seeding, the HES nanocapsules were added to the cell culture (described above). A total of 1 h before the nanocapsules were added to the cell culture, cells were preincubated with folic acid containing DMEM medium in different concentrations (0.1, 0.5, and 1.0 mM) in a humidified incubator. The expression of FRα (on HeLa cells) was confirmed by flow cytometric measurements with a fluorescent allophycocyanin (APC)-conjugated mouse monoclonal antihuman antibody (FOLR1-APC, R&D Systems, U.K.). For CLSM, the cells were analyzed on the ibiTreat μ-slides and washed twice with phosphate-buffered saline without calcium and magnesium (PBS, Invitrogen, Germany) before membrane staining and analysis. For flow cytometry analysis six-well plates were used, the cells were washed with PBS, trypsinized, centrifuged (3 min, 3000 rpm = 956g (m·s^{-2})), and finally resuspended in PBS. The cell viability was confirmed by a MTS assay (CellTiter 96 Aqueous One Solution Cell Proliferation Assay, Promega, U.S.A.), performed according to the product insert in 96-well assay plates (Corning Incorporated costar 3603, Corning, Germany). Each well was populated with 10000 cells the day before the experiment. Absorbance (490 nm) of this assay was measured with a microplate reader (Infinite M1000, Tecan, Switzerland).

Methods of Characterization. The average size and the size distribution of nanocapsules were analyzed by means of dynamic light scattering (DLS) at 25 °C using a Nicomp 380 submicrometer particle sizer equipped with a detector at a 90° angle to the incident beam (Nicomp Particle Sizing Systems, U.S.A.) at 20 °C. The zeta potential of nanocapsules was measured in 10^{-3} M potassium chloride solution with a Nicomp zeta sizer (Nicomp Particle Sizing Systems, U.S.A.) at 20 °C.

The amount of surface-charged groups was calculated from the results of the titration experiments performed on a particle charge detector (Mütek GmbH, Germany) in combination with a Titrino Automatic Titrator (Metrohm AG, Switzerland). The carboxylic groups were titrated against the positively charged polycation poly(diallyl dimethyl ammonium chloride) (poly-DADMAC). The titration was performed on 10 mL of the nanocapsules dispersion with a solid content of 1 g·L^{-1}. The amount of groups per gram of polymer was calculated from the consumed volume of the polyelectrolyte solution. Morphological studies were performed with scanning electron microscopy (SEM). The images were recorded by using a field emission microscope (LEO (Zeiss) 1530 Gemini, Oberkochen, Germany) operated at an accelerating voltage of 170 V. Generally, the samples were prepared by diluting the capsule dispersion in cyclohexane or demineralized water (for redispersed samples) to about 0.01% solid content. A droplet of dispersion was placed onto silica wafers and dried under ambient conditions.

The analysis of the nanocapsules before and after coupling of the folic acid conjugate was performed by FTIR measurements. A total of 3 mg of freeze-dried sample was pressed with KBr to form a pellet and a spectrum between 4000 and 400 cm^{-1} was recorded using the BX spectrometer from Perkin-Elmer. ^{13}C NMR spectra were recorded on a Bruker Avance 300 spectrometer operating with 75 MHz frequency.

The confocal laser scanning microscopy (CLSM) experiments were performed to determine the intracellular localization of the HES nanocapsules. The images were taken using a commercial setup (LSM SP5 STED Leica Laser Scanning Confocal Microscope, Leica, Germany) consisting of an inverse fluorescence microscope DMI 6000 CS equipped with a multilaser combination and five detectors operating in the range of 400−800 nm. A HCX PL APO CS 63×/1.4−0.6 oil-immersion objective was used in these studies. For the excitation of the nanocapsules, a DPSS λ = 561 nm (~20 mW) laser was used. The emission was detected at 580−620 nm. The nanocapsules are pseudocolored in red in the obtained images. The cell membrane was stained with CellMask Deep Red plasma membrane stain (2.5 μg·mL^{-1}, Invitrogen, Germany). In the images, the cell membrane is shown pseudocolored in green (excited with

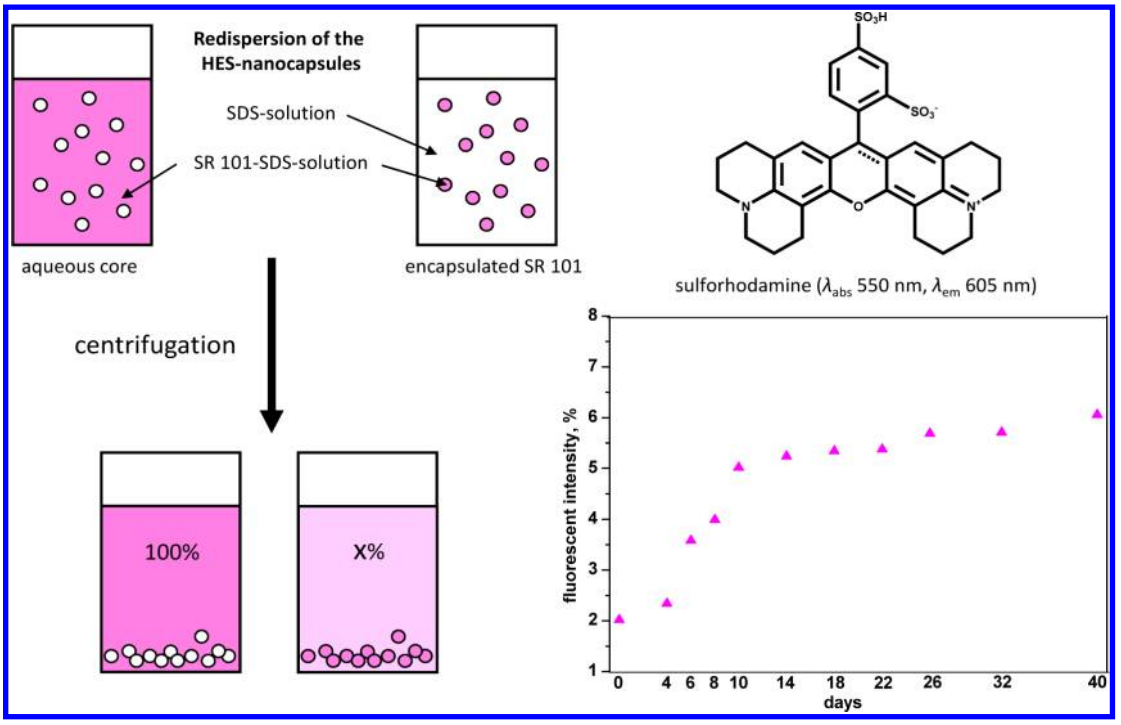

Figure 3. Schematic route of the redispersion process of the HES nanocapsules and the fluorescence intensity of SR101 in the continuous phase after different storage times at 37 °C.

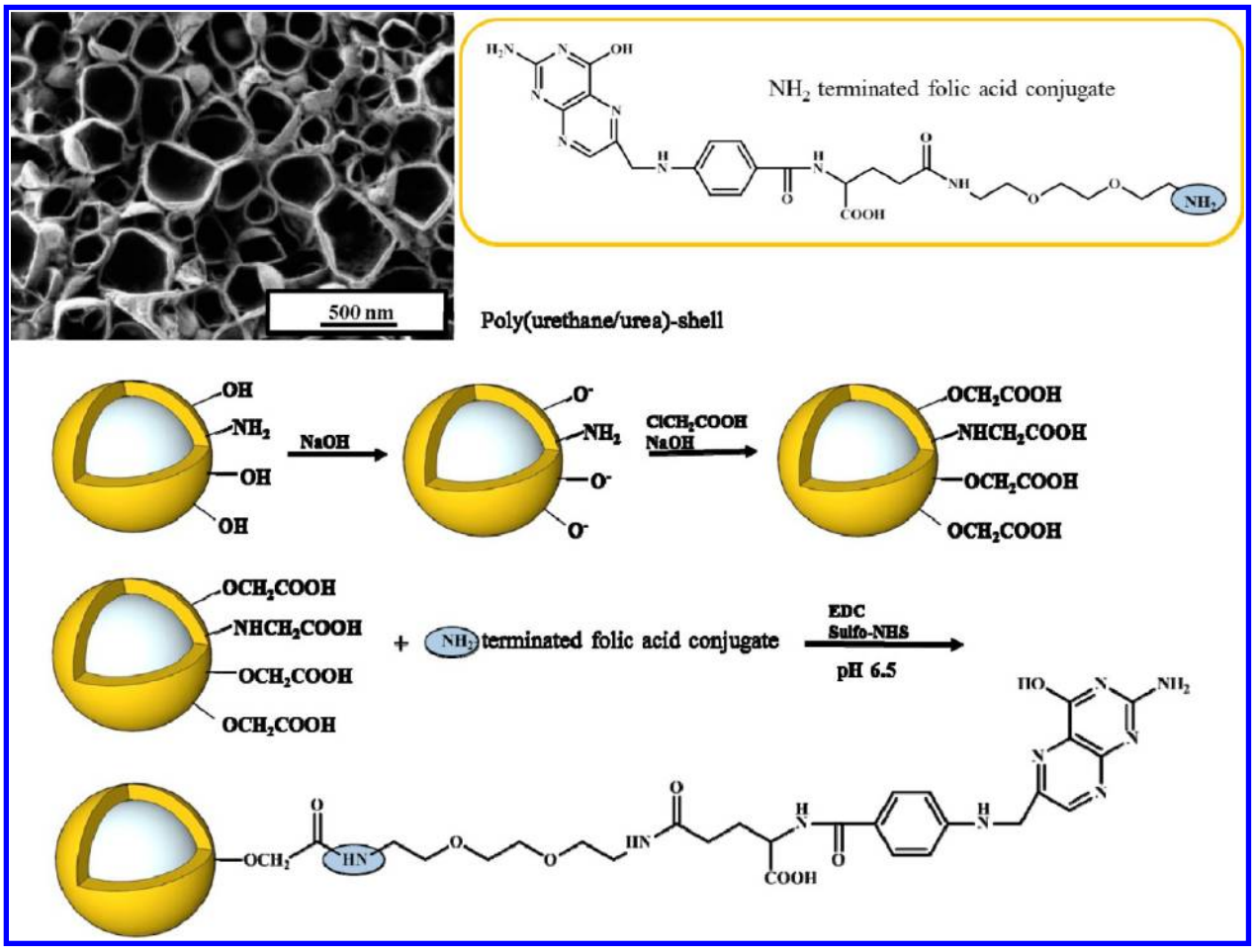

Figure 4. Pathway for the synthesis of folic acid-conjugated HES nanocapsules.

dx.doi.org/10.1021/bm300653v | *Biomacromolecules* 2012, 13, 2704−2715

Table 1. Characterization of the HES Nanocapsules

	HES-cycl (capsules in cyclohexane phase)	HES-R (capsules redispersed in aqueous phase)	HES-CM (capsules after carboxymethylation)	HES-FA (capsules coupled with folic acid)	HES-FA-F (capsules coupled with folic acid after fractionation)
average diameter, nm	275	290	290	307	174
standard deviation, %	28	30	30	31	25
zeta potential at pH 7, mV		−27	−23	−12	−12
covalently attached surface charges, 1/nm^2			0.62	0.14	0.10

HeNe laser: λ = 633 nm ∼10 mW and detected at 660−750 nm). ER-Tracker Green dye Ex/Em 504/511 nm (300 nM) and LysoTracker Green DND-26 Ex/Em 504/511 nm (100 nM), both from Molecular Probes/Invitrogen (Germany), were used for staining of the endoplasmic reticulum (ER) and the lysosomes to analyze the localization of the HES nanocapsules. For the excitation, the Ar laser (∼20 mW, λ = 488 nm) was used, and detection was carried out at 510−550 nm. These compartments are pseudocolored in green, and therefore, the cell membrane is displayed in blue. The measurements, 3D images, and data analyses were performed with the LAS AF program (Leica, Germany). The quantification of the HES nanocapsules' cellular uptake was analyzed by flow cytometry. Measurements were performed with a CyFlow ML using FlowMax 2.57 software (Partec, Germany). SR101-labeled HES nanocapsules were excited with a 561 nm laser, and the fluorescence was detected with a 610−630 nm band-pass filter in the FL5 channel. For the analysis, cells were selected on a forward scatter/sideward scatter plot (488 nm laser), thereby excluding cell debris. These gated events were then further analyzed using the FL5 channel (FCS Express, De Novo Software, U.S.A.). The median in the FL5 was determined from 1D histograms. This corresponds to the amount of nanocapsules taken up or associated with individual cells. All values are triplicates with the standard deviation and confirmed in two independent experiments.

RESULTS AND DISCUSSION

Synthesis and Characterization of Nonfunctionalized and Folic Acid-Conjugated HES Nanocapsules. HES nanocapsules (nonfunctionalized) were synthesized by interfacial polyaddition reaction in the inverse miniemulsion.[31] The synthesis process is shown schematically in Figure 1. The reaction between −OH groups from HES and −NCO groups from TDI occurs at the water-in-oil droplet interface, resulting in the formation of a cross-linked polymeric shell.

The fluorescent dye SR101 was used as a model substance to study the diffusion/permeability of the material through the HES nanocapsule wall. Therefore, the redispersed HES nanocapsules containing SR101 were kept at 37 °C for 40 d. After given periods of time, the HES nanocapsules were precipitated by centrifugation and the amount of released SR101 was determined in the supernatant and compared with the initial value. The results of the fluorescence measurements are shown in Figure 3.

After synthesis and redispersion of the HES nanocapsules in aqueous medium, approximately 2% of the dye was found outside of the capsules, which corresponds to an encapsulation efficiency of 98%. After 10 d it can be noticed that the fluorescence signal increases by 3%. Afterward (until day 40), another increase of 1% was observed. The obtained results indicate that the capsule's polymeric shell possesses high compactness and resistance against leakage over the time.

The amount of used TDI was chosen to be lower than the amount of −OH groups in the HES molecules, and therefore, after redispersion of capsules in the aqueous phase, the residual hydroxyl groups could be converted into carboxylic groups through carboxymethylation. Carboxylic groups were used further for the covalent coupling of amine-terminated folic acid conjugate.

Reaction between the NH_2-terminated folic acid conjugate and carboxyl groups on the nanocapsules surface was achieved using EDC-mediated coupling, which results in the formation of an amide bond (see Figure 4). After the reaction, folate keeps its normal receptor binding affinity due to the introduction of a spacer between the folic acid conjugate and the carboxyl group on the capsule's surface and can therefore be used further in a receptor-mediated endocytosis.[34]

The obtained nanocapsules are colloidal stable and no precipitation or aggregation was observed within 3 months of storage under ambient conditions. SEM studies of HES nanocapsules (Figure 4) confirm the formation of a core−shell structure and the morphology was not changed upon the coupling of folic acid conjugate.

From Figure 4, the amine functionality on the surface can be seen because of residues of unreacted isocyanate groups, which are left on the nanocapsules surface (in cyclohexane). After transferring the nanocapsules into an aqueous phase, the residue of unreacted isocyanate groups totally disappears. This shows that a hydrolysis reaction occurs between isocyanate groups and water to form amine groups via the formation of an unstable carbamic acid intermediate.

HES nanocapsules before and after functionalization with folic acid conjugate were characterized in terms of average size, electrokinetic potential (zeta potential), and the number of surface charges before and after the coupling of folic acid conjugate was determined. The characteristics of the nanocapsules after the synthesis (sample HES-Cycl), after redispersion in an aqueous phase (sample HES-R), after carboxymethylation (sample HES-CM), and after the coupling of folic acid conjugate (samples HES-FA and HES-FA-F) are summarized in Table 1. The DLS curves of sample HES-FA (left, capsules coupled with folic acid) and HES-FA-F (right, capsules coupled with folic acid after fractionation) are shown in the Supporting Information as representative examples, see Figure S1.

After synthesis, the average size of the nanocapsules was about 275 nm. The size of nanocapsules after redispersion and carboxymethylation procedures slightly increases, which could be due to the surface-attached hydration layer. The coupling of folic acid conjugate results in a further size increase to 307 nm. The size polydispersity (standard deviation) stays approximately (around 30%) the same for all described samples. The obtained values and SEM observations (Figure 4) reveal the presence of large and small capsules. To study the effect of capsule size on the cell uptake behavior, the sample HES-FA (after coupling of folic acid conjugate) was fractionated by

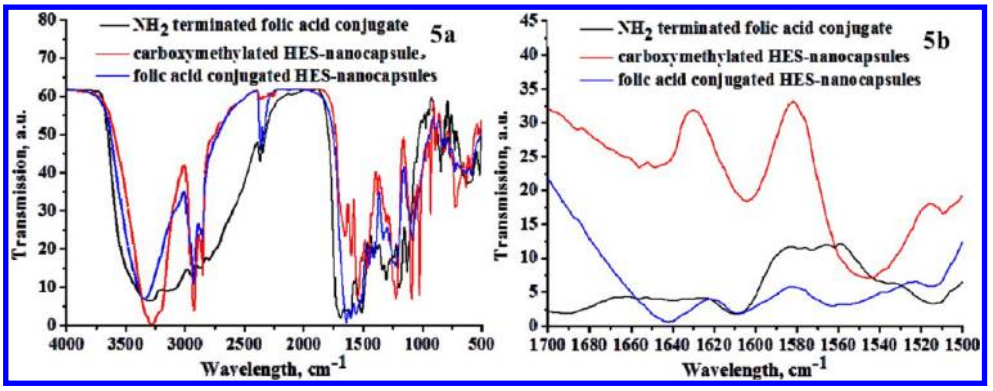

Figure 5. (a) FT-IR spectra of NH_2-terminated folic acid conjugate (in black), carboxymethylated HES nanocapsules (in red), and folic acid-conjugated HES nanocapsules (in blue); (b) Section of the region 1700−1500 cm^{-1}.

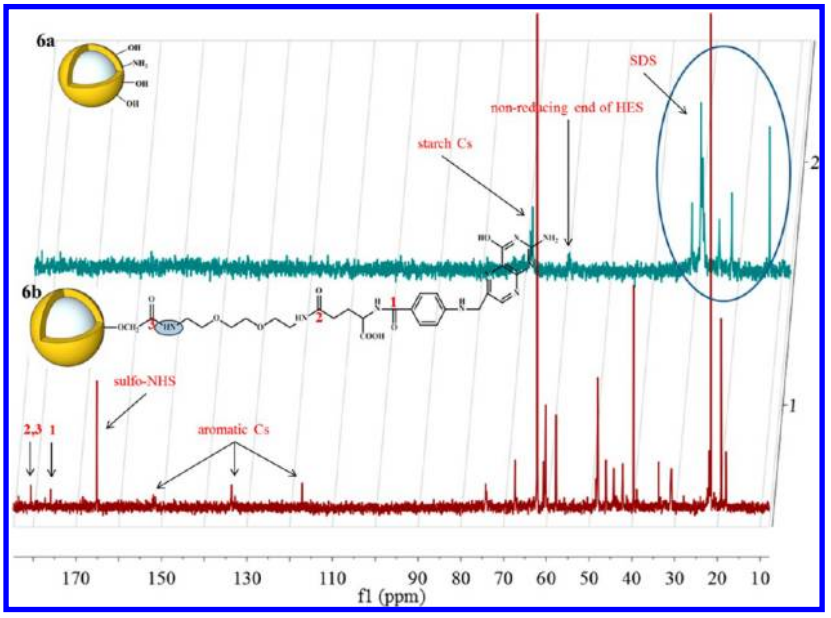

Figure 6. ^{13}C NMR spectra (D_2O-d_6) of the redispersed HES nanocapsules (HES-R, a) and the folic acid-conjugated HES nanocapsules (HES-FA, b).

centrifugation to separate small capsules (about 70 vol %), which were further used in the cell experiments.

The zeta potential of the redispersed and dialyzed HES nanocapsules is negative (−27 mV) due to the presence of anionic surfactant used for the redispersion process (SDS-solution 0.1 wt %). After coupling of the folic acid conjugate the zeta potential increases to −12 mV. The amount of covalently attached ionic groups per nanocapsule was calculated from the results of particle charge titration as a difference in the volume of polyelectrolyte, which was consumed at pH 10 (carboxylic and sulfate groups are deprotonated) and at pH 2.5 (only sulfate groups are deprotonated).[40] The titration of carboxymethylated nanocapsules revealed that there are approximately 0.62 groups per nm^2. After the coupling and fractionation procedure, the concentration of negatively charged groups reduces up to 0.14 and 0.10 groups per nm^2 for the samples HES-FA and HES-FA-F, respectively. The lower density of anionic groups in comparison to the sample after carboxymethylation could be due to the "shielding" of the negative carboxylic/sulfate charges by positive ammonium groups, originated from the folic acid conjugate.

The chemical composition of HES nanocapsules was studied by FTIR spectroscopy (see Figure 5). The covalent coupling of folic acid conjugate onto HES nanocapsules surface was additionally investigated using ^{13}C NMR, see Figure 6. FT-IR spectroscopy was performed on dried HES nanocapsules from the cyclohexane phase to identify the chemical reaction between the COOH and NH_2 groups leading to an amide bond formation. The complete IR spectra and the section of characteristic bands after coupling of NH_2 terminated folic acid conjugate to the carboxymethylated HES nanocapsules are shown in Figure 5a and b, respectively.

The IR spectrum of the folic acid conjugate (Figure 5a, black line) shows various functional groups of the molecule. The vibration bands at 1635 and 1554 cm^{-1} indicate a successful folic acid binding (see Figure 5b). The red line in Figure 5a corresponds to the IR spectra of the carboxymethylated HES nanocapsules. A strong band which is characteristic for the oxygen-bonded O−H stretching vibration (3450 cm^{-1}) and for the N−H valence vibration (3300 cm^{-1}) can be seen. The C−H valence vibration of the aromatic system is around 2850 cm^{-1}. The characteristic bands for the urethane (1720 and 1700 cm^{-1}) and urea (1670 cm^{-1}) units can be assigned as well. The two bands at 1720 and 1700 cm^{-1} result from the C═O vibration. The band at 1720 cm^{-1} results from the free C═O and the one at 1700 cm^{-1} from the polyurethane.[41] After the

coupling of NH_2-terminated folic acid conjugate with the carboxymethylated HES nanocapsules, the characteristic bands of carboxymethylated HES nanocapsules and those of folic acid could be seen (Figure 5b in blue). The characteristic bands at 1635 cm^{-1} corresponds to −CONH amide band and at 1554 cm^{-1} corresponds to −NH amide band. Furthermore, the absorption of the amide band (at 1635 cm^{-1}) increases, which is due to the linkage between the NH_2 group of the folic acid conjugates and the COOH group of the carboxymethylated HES nanocapsules.

As a further proof for the covalent binding of the folic acid molecule to the nanocapsules, NMR spectroscopy was used. The peaks of the surfactant were observed in the NMR spectrum of the redispersed HES nanocapsules (Figure 6a) between 10 and 35 ppm.[42] The peak at about 60 ppm originates from the nonreducing end of the hydroxyethyl starch and the peak at about 70 ppm contributes to the $-CH_2-O-$ moieties.[43] In the spectrum of the folic acid-conjugated HES nanocapsules (Figure 6b), the peaks in the range between 0 and 75 ppm result on one hand from the residuals of the coupling procedure (EDC and S-NHS) and from the folic acid conjugate. On the other hand, the peaks are assigned to originate from the surfactant and from the HES in the same manner as described for the spectrum in Figure 6a. The signals between 115 and 155 ppm are from the aromatic carbons of the coupled folic acid conjugate. Additional peaks at 170−180 ppm can be assigned to amide carbonyl atoms.

The total amount of the folic acid attached to the HES nanocapsules was determined using fluorescence spectroscopy; see 3D scan in the Supporting Information (Figure S3). The results for the total amount of the folic acid attached to the HES nanocapsules were evaluated by measuring the fluorescence intensity at 365 and 445 nm. The amount of the NH_2-terminated folic acid conjugate detected in the supernatant was about 45 wt %. This means that about half the amount of the introduced folic acid conjugate was attached onto the capsule surface, involving participation of almost all carboxylic surface groups in the coupling reaction.

Cellular Uptake of Redispersed and Folic Acid-Conjugated HES Nanocapsules. Several initial experiments with HeLa cells in standard DMEM medium showed that the intracellular uptake of the folic acid-conjugated HES nanocapsules (HES-FA) is higher than the uptake of HES nanocapsules after redispersion (HES-R). For further experiments, FRα expressing HeLa cells and FRα[44,45] nonexpressing A549 cells[46,47] were chosen as model cells to investigate whether a folate receptor-mediated (specific) or a nonspecific cell uptake plays a decisive role in the internalization of HES redispersed in water (HES-R) and HES-coupled (HES-FA) nanocapsules. Before performing further experiments, the HES nanocapsules were checked for potential cytotoxicity by using the MTS assay. The metabolic activity of the cells was not significantly reduced after incubation with HES redispersed (HES-R) and HES coupled (HES-FA) samples for 24 h. The expression of the folate receptor (FRα) was confirmed for HeLa cells, and A549 cells were approved as FRα nonexpressing cells (data not shown). Additional folic acid in the cell culture medium could competitively inhibit a folate receptor-mediated uptake of nanoscaled formulations.[45,47,48] Therefore, the succeeding experiments with the HeLa cells were performed with additional folic acid (0.1, 0.5, and 1.0 mM) in the cell medium to analyze the influence of a folate receptor-mediated uptake. An observation time of 24 h was selected to facilitate a maximum nonspecific uptake,[47] while shorter observation times might favor FRα-mediated uptake. Therefore, an uptake experiment over 2 h with HES nanocapsules was conducted with HeLa cells as well. The effect of nanocapsules size on the cell uptake was studied with two samples of folic acid-conjugated HES capsules. One sample (HES-FA) with an average size of 307 nm and second sample (HES-FA-F) was a fraction of smaller capsules (174 nm) obtained after centrifugation of the sample HES-FA. HeLa and A549 cells were cultured (see Experimental Section) in a folic acid-free cell culture medium for four days before the HES nanocapsules were added to the cell culture (for details see Experimental Section, Cell Culture). Due to the lack of folic acid in the medium, FRα positive cells (HeLa cells) were expected to increase the FRα expression on the cell surface.[48−50] The preincubation for 1 h with a folic acid-containing cell culture medium (samples were exposed to different concentrations of folic acid: 0.1, 0.5, and 1.0 mM) was expected to block the folic acid receptors on the cell surface and, hence, inhibit a potential folic acid receptor-mediated uptake route.[45,48] The experiments with FRα-positive HeLa cells were carried out with different folic acid concentrations for 2 and 24 h simultaneously (see Figure 7).

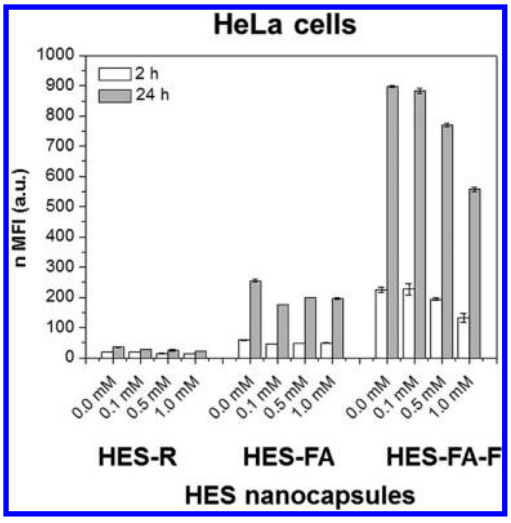

Figure 7. Cellular uptake in HeLa cells of HES-R, HES-FA, and HES-FA-F nanocapsules after 2 and 24 h. Nanocapsule incubation was performed without additional folic acid (0.0 mM) and with 0.1, 0.5, and 1.0 mM folic acid in DMEM medium. Flow cytometric measurements show the normalized median of the fluorescence intensity (nMFI, normalized to nanocapsules per mL) in arbitrary units (a.u.) and the standard deviation (all values are gained from dual approaches).

In general, HeLa cells showed a very low cellular uptake for HES-R. A considerable uptake was shown for HES-FA (compared to HES-R without additional folic acid (0.0 mM): 3 times higher after 2 h and 7 times higher after 24 h) and a high one for HES-FA-F (compared to HES-R without additional folic acid (0.0 mM): 11 times higher after 2 h and 25 times higher after 24 h). The cellular uptake after 24 h was less than doubled on a very low level compared to the results after 2 h for HES-R. For HES-FA and HES-FA-F there was a 4-fold increased (approximately). An uptake inhibition caused by the additional folic acid was not recognized for HES-R and HES-FA, but for HES-FA-F with increased folic acid

concentrations of 0.5 and 1.0 mM. The uptake of HES-FA-F is reduced by about one-third (sample with 1.0 mM folic acid), compared to the folic acid-free sample (0.0 mM). The control experiment with FRα-negative A549 cells was performed within 24 h and is shown in Figure 8.

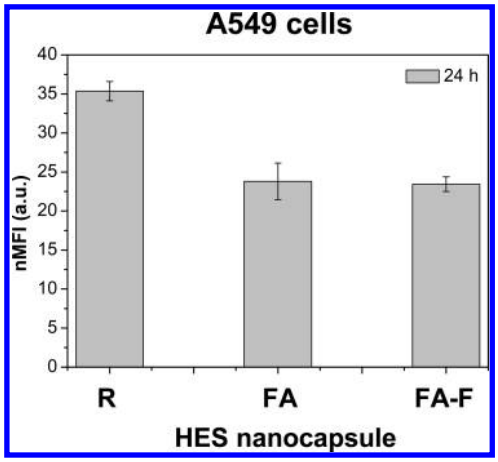

Figure 8. Cellular uptake in A549 cells of HES-R, HES-FA, and HES-FA-F nanocapsules after 24 h. The incubation was performed without additional folic acid in DMEM medium. The flow cytometric measurements show the normalized median of the fluorescence intensity (nMFI, normalized to nanocapsules per mL) in arbitrary units (a.u.) and the standard deviation (all values are gained from dual approaches).

A very low cellular uptake in A549 cells was detectable for HES-R, HES-FA, and HES-FA-F (compare nMFI values for Figures 7 and 8). Differences between HES-R, HES-FA, and HES-FA-F are not relevant compared to the results of Figure 7 and may be due to slight differences in the steps between different modifications of the nanocapsules. Therefore, coupling of FA did not enhance significantly the uptake of HES nanocapsules. In conclusion, the average size of HES nanocapsules plays an important role in the quantitative uptake into HeLa cells. The folic acid-conjugated HES nanocapsules with smaller size (HES-FA-F, 174 nm) show a quantitatively better uptake than HES-FA with an average size of 307 nm. Also, longer incubation periods provide a more quantitative cellular uptake in HeLa cells (drastic increase between 2 and 24 h in HeLa cells). Only the uptake of the smaller folic acid-conjugated HES-FA-F nanocapsules could be partially inhibited by additional folic acid. This gives a strong hint for a size-dependent FRα-mediated uptake of folic acid-conjugated HES nanocapsules. A partial inhibition of FRα-mediated endocytosis with additional folic acid was proven for different folate-conjugated nanoparticles of various materials in HeLa cells by other groups before.[48,51] The inhibition efficiency cannot be directly compared due to differences in the experimental setup (nanomaterials, concentrations, incubation periods, etc.), but a complete suppression of cellular uptake never occurred. A FRα-mediated uptake is accompanied with other cellular uptake mechanisms. Detailed information about the intracellular localization of HES-R, HES-FA, and HES-FA-F nanocapsules in HeLa and A549 cells was obtained by CLSM measurements (Figures 9 and 10). The intracellular uptake after 24 h in HeLa cells is shown in Figure 9.

Obviously the intracellular uptake of HES-R, HES-FA, and HES-FA-F nanocapsules did not lead to any morphological changes to the HeLa cells compared to the untreated ones. The images clearly give evidence of a higher intracellular uptake of HES-FA and HES-FA-F (images C–F) in comparison to HES-R, where only a very low uptake is detected inside the cells (images A and B). The results of the flow cytometric measurements are confirmed regarding the effect of the folate conjugation on the nanocapsules surface. The HES nanocapsules are not single-dispersed in the cytoplasm but rather located together with other nanocapsules. An uptake inhibition induced by additional 1.0 mM folic acid could be surmised but not definitely determined by visual inspection of the CLSM images. There are some attachments of HES nanocapsules visible on the cellular membrane/cell surface (overlay of green-colored cellular membrane and the red-colored nanocapsules resulting in yellow stained areas). Additionally, the CLSM images for the incubation in A549 cells are shown in Figure 10 after 24 h.

For all samples (Figure 10) incubated with redispersed (HES-R, image A) and folic acid-conjugated (HES-FA and HES-FA-F, images B and C) HES nanocapsules, only a marginal intracellular uptake was detectable. In accordance with flow cytometric measurements (Figure 8), no uptake enhancement caused by coupling of FA or size fractioning was observed in FRα nonexpressing A549 cells. For HES-R (Figure 10A) and

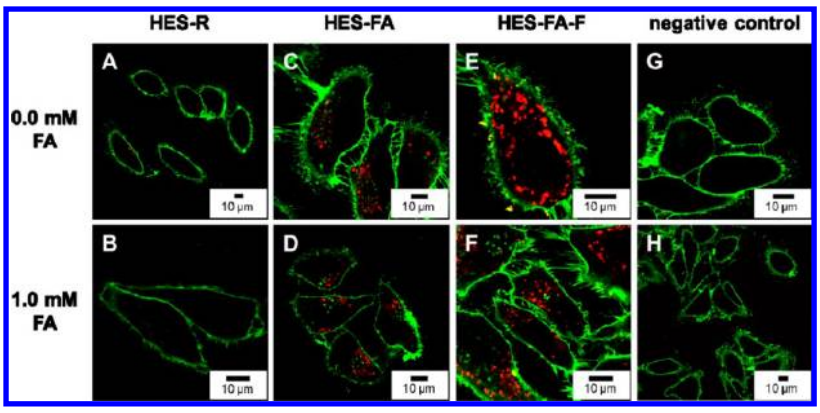

Figure 9. CLSM images of HeLa cells after incubation with HES-R (A, B), HES-FA (C, D), and HES-FA-F (E, F) nanocapsules and the negative control (NC) without nanocapsules (G, H) after 24 h: first row, HeLa cells without additional folic acid (0.0 mM) in the cell culture medium; second row, HeLa cells with additional folic acid (1.0 mM) in the cell culture medium. HES nanocapsules are pseudocolored in red, cell membrane in green (CellMask Deep Red).

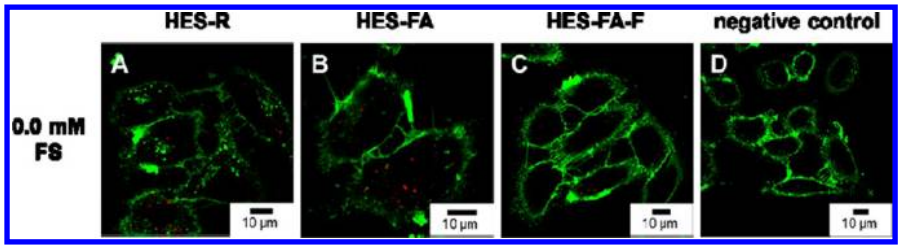

Figure 10. CLSM images of A549 cells without additional folic acid (0.0 mM) in the cell culture medium after incubation (24 h) with HES-R (A), HES-FA (B), and HES-FA-F (C) nanocapsules and the negative control (NC) without nanocapsules (D). HES nanocapsules are pseudocolored in red and cell membrane is in green (CellMask Deep Red).

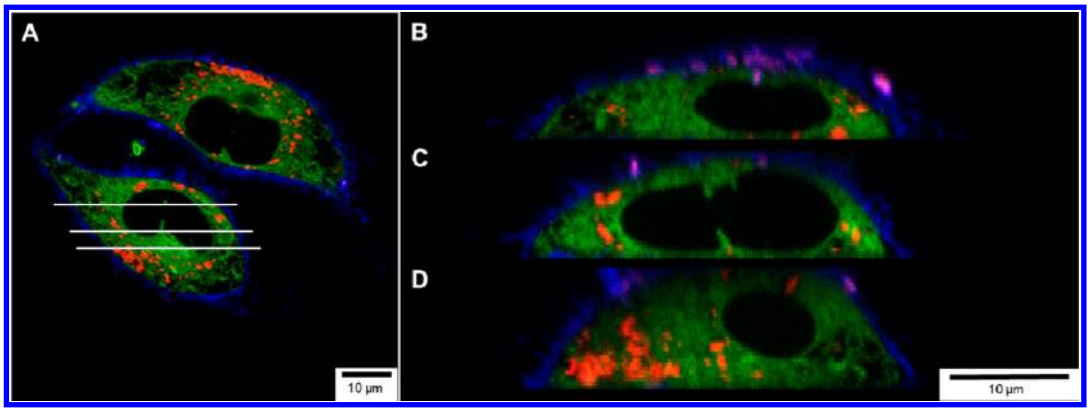

Figure 11. CLSM image: Intracellular localization of HES-FA-F nanocapsules in HeLa cells (A) after 24 h. Horizontal cross sections (B), (C), and (D) are approximately indicated by white lines. The cell membrane is pseudocolored in blue (CellMask Deep Red), HES-FA-F in red, and the ER in green.

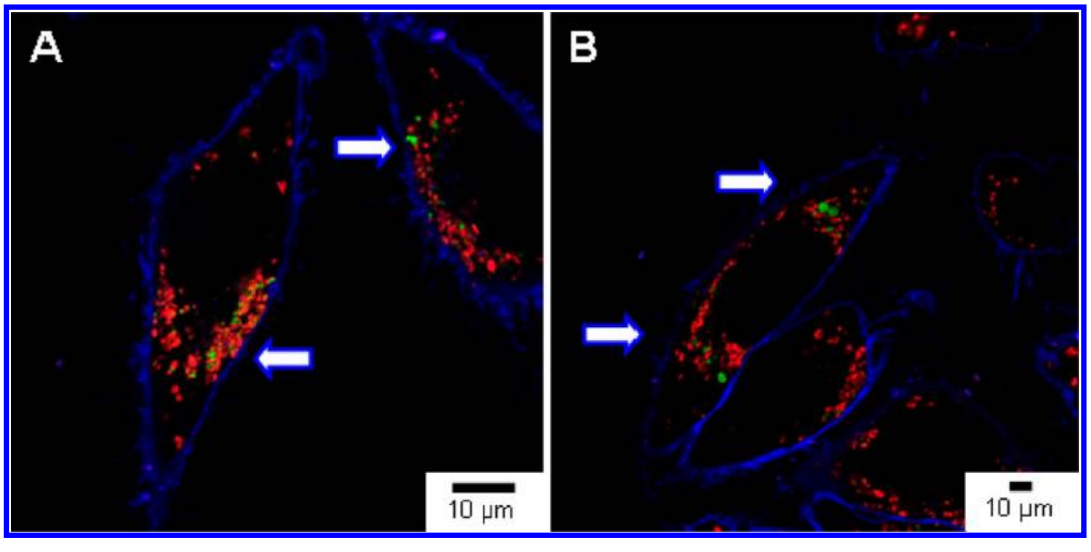

Figure 12. CLSM image: Colocalization studies of HES-FA-F nanocapsules and lysosomes (white arrows) in HeLa cells after 20 h (A) and 40 h (B). The cell membrane is pseudocolored in blue (CellMask Deep Red), HES-FA-F in red, and the lysosomes in green.

HES-FA (Figure 10B), no significant difference in uptake is detectable. Notably, there is a small uptake of HES-R and HES-FA visible in our LSM studies. Also, for HES-FA-F there is a detectable uptake that is even less obvious, as the smaller sizes also show a lower intensity per pixel and therefore are not so prominent in Figure 10C. The explanation therefore is most probably that also unspecific mechanisms of uptake that do not involve a specific receptor are active in these cells and presumably also other cell lines. The reader is pointed toward a broad literature of our group and others where uptake is influenced by particle surface and other factors like shape with no specific ligands involved.[32,52,53] Different to other drug delivery systems like liposomes or vesicles, where internalized components are trafficked to lysosomes, folate-conjugated substrates, which are taken up via FRα-mediated endocytosis, are known to end up in endocytotic compartments or are released into the cytoplasm. To continue the studies, further colocalization studies have been carried out to obtain more information about the intracellular localization of the HES nanocapsules. The endoplasmic reticulum (ER) and the lysosomes were stained with ER-Tracker Green dye and LysoTracker Green DND-26, respectively. The folic acid-

dx.doi.org/10.1021/bm300653v | *Biomacromolecules* 2012, 13, 2704−2715

conjugated HES nanocapsules (HES-FA-F) showed a preferred localization next to the endoplasmic reticulum (ER), but they did not touch the nucleus (surrounded by the ER) itself (see Figure 11). That could be caused by the size of the intracellular nanocapsule accumulations, which prevent a closer approach to the nucleus. A colocalization of green ER and red HES-FA-F nanocapsules would have been displayed in yellow and was not expected and not detected in any image of this study. Attachments of HES-FA-F to the cell membrane could be seen especially in the cross sections B and C (rose-overlay of the blue cell membrane and the red (HES-FA-F) nanocapsules).

To obtain further evidence about the intracellular fate of HES-FA-F, a colocalization study was performed with a lysosomal marker (see Figure 12).

Neither after 20 h nor after 40 h could a yellow colocalization of red (HES-FA-F) and green lysosomes be detected (Figure 12). This fact leads to the conclusion that the intracellular accumulations of HES-FA-F do not end up in lysosomes. The final destination in intracellular vesicles or the storage in other endosomes/endocytic compartments, entrapped there after folate receptor-mediated uptake, seems to be more reasonable.

CONCLUSION

In the present work, polymeric hydroxyethyl starch (HES) nanocapsules were synthesized using the inverse (water-in-oil) miniemulsion process. The capsules have a spherical shape with "core-shell" morphology and an average size of 275 nm. After synthesis and redispersion of the capsules in the aqueous phase, a NH_2-terminated folic acid conjugate was covalently bound to the carboxyl-functionalized surface through EDC-mediated coupling. The successful coupling was proved by FT-IR and NMR spectroscopies, and the amount of attached folic acid conjugate was determined from the fluorescence intensity data.

After coupling of folic acid, it was possible to obtain two fractions of the capsules with smaller and larger diameters using centrifugation. The HES nanocapsules before and after coupling were subjected to cell uptake experiments. Very low cellular uptake was observed with HES nanocapsules, which were redispersed in aqueous medium and not subjected to any further surface modifications. Conjugation with a folic acid conjugate enabled a specific cellular uptake of the capsules into HeLa cells. A549 cells showed a very low cellular uptake for both nonfunctionalized and folic acid-conjugated HES nanocapsules. A FRα-mediated uptake in HeLa cells was confirmed (especially for HES nanocapsules of a lower size fraction or with an average size of around 174 nm) and partially inhibited for this smaller fraction when additional folic acid was present in the cell culture medium. The results of the presented studies could be of high interest for the development of receptor-mediated targeting using polymeric nanocapsules to deliver and accumulate their encapsulated molecules to the target area.

ASSOCIATED CONTENT

Supporting Information

Dynamic light scattering graphs, ^{1}H NMR spectra, and a 3D fluorescence scan. This material is available free of charge via the Internet at http://pubs.acs.org.

AUTHOR INFORMATION

Corresponding Author

*E-mail: landfester@mpip-mainz.mpg.de. Tel.: +49(0)6131 379-170. Fax: +49(0)6131 379-370.

Notes

The authors declare no competing financial interest.

ACKNOWLEDGMENTS

The authors thank Gunnar Glasser for his help in SEM imaging.

REFERENCES

(1) Low, P. S.; Kularatne, S. A. *Curr. Opin. Chem. Biol.* **2009**, *13* (3), 256−262.
(2) Sega, E. I.; Low, P. S. *Cancer Metast. Rev.* **2008**, *27* (4), 655−664.
(3) Sun, C.; Sze, R.; Zhang, M. *J. Biomed. Mater. Res., Part A* **2006**, *78* (3), 550−557.
(4) Sudimack, J.; Lee, R. J. *Adv. Drug Delivery Rev.* **2000**, *41* (2), 147−162.
(5) Sahu, S. K.; Mallick, S. K.; Santra, S.; Maiti, T. K.; Ghosh, S. K.; Pramanik, P. *J. Mater. Sci.: Mater. Med.* **2010**, *21* (5), 1587−1597.
(6) Kelemen, L. E. *Int. J. Cancer* **2006**, *119* (2), 243−250.
(7) Narayanan, S.; Binulal, N. S.; Mony, U.; Manzoor, K.; Nair, S.; Menon, D. *Nanotechnology* **2010**, *21*, 28.
(8) Gabizon, A.; Horowitz, A. T.; Goren, D.; Tzemach, D.; Mandelbaum-Shavit, F.; Qazen, M. M.; Zalipsky, S. *Bioconjugate Chem.* **1999**, *10* (2), 289−298.
(9) Hayama, A.; Yamamoto, T.; Yokoyama, M.; Kawano, K.; Hattori, Y.; Maitani, Y. *J. Nanosci. Nanotechnol.* **2008**, *8* (6), 3085−3090.
(10) Bae, Y.; Jang, W. D.; Nishiyama, N.; Fukushima, S.; Kataoka, K. *Mol. Biosyst.* **2005**, *1* (3), 242−250.
(11) Stella, B.; Arpicco, S.; Peracchia, M. T.; Desmaele, D.; Hoebeke, J.; Renoir, M.; D'Angelo, J.; Cattel, L.; Couvreur, P. *J. Pharm. Sci.* **2000**, *89* (11), 1452−1464.
(12) Esmaeili, F.; Ghahremani, M. H.; Ostad, S. N.; Atyabi, F.; Seyedabadi, M.; Malekshahi, M. R.; Amini, M.; Dinarvand, R. *J. Drug Target.* **2008**, *16* (5), 415−423.
(13) Garcia-Bennett, A.; Nees, M.; Fadeel, B. *Biochem. Pharmacol.* **2011**, *81* (8), 976−984.
(14) Singh, R.; Lillard, J. W. *Exp. Mol. Pathol.* **2009**, *86* (3), 215−223.
(15) Wang, X.; Shen, F.; Freisheim, J. H.; Gentry, L. E.; Ratnam, M. *Biochem. Pharmacol.* **1992**, *44* (9), 1898−1901.
(16) Webster, R.; Elliott, V.; Park, B. K.; Walker, D.; Hankin, M.; Taupin, P. *Milestones Drug Ther.* **2009**, 127−146.
(17) Besheer, A.; Vogel, J.; Glanz, D.; Kressler, J.; Groth, T.; Mader, K. *Mol. Pharm.* **2009**, *6* (2), 407−415.
(18) Marchant, R. E.; Yuan, S.; Szakalasgratzl, G. *J. Biomater. Sci., Polym. Ed.* **1994**, *6* (6), 549−564.
(19) Osterberg, E.; Bergstrom, K.; Holmberg, K.; Schuman, T. P.; Riggs, J. A.; Burns, N. L.; Vanalstine, J. M.; Harris, J. M. *J. Biomed. Mater. Res.* **1995**, *29* (6), 741−747.
(20) Haass, A.; Treib, J.; Pindur, G.; Krack, P.; Wenzel, E.; Schimrigk, K. *Naunyn-Schmiedeberg's Arch. Pharmacol.* **1989**, *339* (Suppl), R117.
(21) Kiesewetter, H.; Erlenwein, S.; Jung, F.; Wenzel, E.; Vogel, W.; Dyckmans, J.; Bach, R.; Hahmann, H.; Schieffer, H.; Bette, L. *Klin. Wochenschr.* **1988**, *66* (Suppl.15), 8−14.
(22) Kiesewetter, H.; Jung, F.; Blume, J.; Gerhards, M. *Klin. Wochenschr.* **1987**, *65* (7), 324−330.
(23) Jesch, F.; Hubner, G.; Zumtobel, V.; Zimmermann, M.; Messmer, K. *Infus. Ther. Transfus.* **1979**, *6* (2), 112−117.
(24) Yoshida, M.; Kishikawa, T. *Stärke* **1984**, *36* (5), 167−169.
(25) Yoshida, M.; Yamashit., T; Matsuo, J.; Kishikawa, T. *Stärke* **1973**, *25* (11), 373−376.
(26) Förster, H. *Hämorheol. Operat. Med.* **1988**, 118−134.
(27) Devy, J.; Balasse, E.; Kaplan, H.; Madoulet, C.; Andry, M. C. *Int. J. Pharm.* **2006**, *307* (2), 194−200.
(28) Bajpai, A. K.; Bhanu, S. *J. Mater. Sci.: Mater. Med.* **2007**, *18* (8), 1613−1621.
(29) Balasse, E.; Odot, J.; Gatouillat, G.; Andry, M. C.; Madoulet, C. *Int. J. Pharm.* **2008**, *353* (1−2), 131−138.
(30) Henrist, D.; Lefebvre, R. A.; Remon, J. P. *Int. J. Pharm.* **1999**, *187* (2), 185−191.

(31) Baier, G.; Musyanovych, A.; Dass, M.; Theisinger, S.; Landfester, K. *Biomacromolecules* **2010**, *11* (4), 960−968.
(32) Paiphansiri, U.; Dausend, J.; Musyanovych, A.; Mailander, V.; Landfester, K. *Macromol. Biosci.* **2009**, *9* (6), 575−584.
(33) Leamon, C. P.; Pastan, I.; Low, P. S. *J. Biol. Chem.* **1993**, *268* (33), 24847−24854.
(34) Lee, R. J.; Low, P. S. *J. Biol. Chem.* **1994**, *269* (5), 3198−3204.
(35) Weitman, S. D.; Lark, R. H.; Coney, L. R.; Fort, D. W.; Frasca, V.; Zurawski, V. R.; Kamen, B. A. *Cancer Res.* **1992**, *52* (12), 3396−3401.
(36) Schlaad, H.; Kukula, H.; Rudloff, J.; Below, I. *Macromolecules* **2001**, *34* (13), 4302−4304.
(37) Crespy, D.; Landfester, K. *Macromol. Chem. Phys.* **2007**, *208* (5), 457−466.
(38) Landfester, K.; Musyanovych, A.; Mailänder, V. *J. Polym. Sci., Polym. Ed.* **2009**, *48* (3), 493−515.
(39) Zhang, Z. P.; Lee, S. H.; Feng, S. S. *Biomaterials* **2007**, *28* (10), 1889−1899.
(40) Cuba-Chiem, L. T.; Huynh, L.; Ralston, J.; Beattie, D. A. *Langmuir* **2008**, *24* (15), 8036−8044.
(41) Zanetti-Ramos, B. G.; Lemos-Senna, E.; Soldi, V.; Borsali, R.; Cloutet, E.; Cramail, H. *Polymer* **2006**, *47* (24), 8080−8087.
(42) Varshney, M. *Colloid Surf., A* **1995**, *96* (3), 273−275.
(43) Tavares, M. I. B.; Bathista, A.; Silva, E. O.; Costa, P. M.; Filho, N. P.; Nogueira, J. S. *J. Appl. Polym. Sci.* **2004**, *92* (4), 2151−2154.
(44) Zhang, Z.; Jia, J.; Lai, Y.; Ma, Y.; Weng, J.; Sun, L. *Bioorg. Med. Chem.* **2010**, *18* (15), 5528−5534.
(45) Zhang, P.; Zhang, Z.; Yang, Y.; Li, Y. *Int. J. Pharm.* **2010**, *392* (1−2), 241−248.
(46) Bharali, D. J.; Lucey, D. W.; Jayakumar, H.; Pudavar, H. E.; Prasad, P. N. *J. Am. Chem. Soc.* **2005**, *127* (32), 11364−11371.
(47) Eisele, K.; Gropeanu, R.; Musante, A.; Glasser, G.; Li, C.; Muellen, K.; Weil, T. *Macromol. Rapid Commun.* **2010**, *31* (17), 1501−1508.
(48) Zhang, B. L.; Li, Y. Q.; Fang, C. Y.; Chang, C. C.; Chen, C. S.; Chen, Y. Y.; Chang, H. C. *Small* **2009**, *5* (23), 2716−2721.
(49) Leamon, C. P.; Low, P. S. *Proc. Natl. Acad. Sci. U.S.A.* **1991**, *88* (13), 5572−5576.
(50) Tavares, S.; Sousa, J.; Goncalves, P.; Araujo, J. R.; Martel, F. *Eur. J. Pharmacol.* **2010**, *640* (1−3), 29−37.
(51) Zhang, P. C.; Zhang, Z. W.; Yang, Y. X.; Li, Y. P. *Int. J. Pharm.* **2010**, *392* (1−2), 241−248.
(52) Weiss, C. K.; Lorenz, M. R.; Landfester, K.; Mailander, V. *Macromol. Biosci.* **2007**, *7* (7), 883−896.
(53) Lorenz, M. R.; Kohnle, M. V.; Dass, M.; Walther, P.; Höcherl, A.; Ziener, U.; Landfester, K.; Mailander, V. *Macromol. Biosci.* **2008**, *8* (8), 711−727.